Plasma Simulation of the Micro-Vacuum Arc Thruster Based on PIC

IEPC-2017-459

Presented at the 35th International Electric Propulsion Conference
Georgia Institute of Technology • Atlanta, Georgia • USA
October 8 – 12, 2017

Song Bai[1], Kan Xie[2,*], Qimeng Xia[3], Zun Zhang[4], Ningfei Wang[5]
Beijing Institute of Technology, Beijing, 100081, China

Xianming Wu[6], Ning Guo[7]
National key laboratory of Science and Technology on Vacuum Technology &Physics, Lanzhou, 730000, China

Abstract: The micro-vacuum arc thruster is a kind of micro-thruster based on an ablative vacuum arc technology. It's uniquely suitable for small satellite missions because of its simplicity, economy and reliability. However, the plasma diagnosis in such a narrow region is complicated and not appropriate. In this paper, a 2-D axisymmetric model was built and a numerical analysis based on PIC method was performed to study the plasma plume of the thruster. The structure of the plasma plume is investigated, and then the influences of the magnetic field intensity on the plasma plume are discussed. Additionally, the results of the ring-electrodes μVAT are compared with those of the co-axial μVAT.

Nomenclature

$\boldsymbol{B}$	=	magnetic field vector
$\boldsymbol{E}$	=	electric field vector
$\boldsymbol{v}$	=	particle velocity vector
$\boldsymbol{x}$	=	particle position vector
m	=	particle mass
q	=	particle charge
ε	=	vacuum permittivity
ρ	=	grid charge density
ϕ	=	potential
t	=	time
r, z, θ	=	radial, axial and circular position
V_{i0}	=	initial velocity of ions
V_{ir}, V_{iz}, $V_{i\theta}$	=	components of initial velocity of ions
Δt	=	time step
Δx	=	grid size

[1] Doctoral student, School of Aerospace Engineering, aaarko0@gmail.com.
[2] Associate professor, School of Aerospace Engineering, xiekan@bit.edu.cn.
[3] Doctoral student, School of Aerospace Engineering, xiaqimengbit@gmail.com.
[4] Postdoctoral student, School of Physics, zhangzun@bit.edu.cn.
[5] Professor, School of Aerospace Engineering, wangningfei@bit.edu.cn.
[6] Senior engineer, Electric Propulsion Department, wxm0511@163.com.
[7] Associate researcher, Electric Propulsion Department, guoningaa@163.com.

I.Introduction

The CubeSat is more and more widely used in space missions due to its simplicity, economy and reliability[1]. However, because of the small volume and mass, most CubeSats cannot equip an efficient propulsion system, resulting in a relatively short lifetime and affecting the application of the CubeSat[2]. The Micro-Vacuum Arc Thruster (μVAT) is a novel micro-propulsion device developed in recent years. By adapting the simple technology of an inductive energy storage circuit PPU and the "triggerless" ignition method[3], the mass of the propulsion system can be lower than 200g, with a specific impulse of >1000s and a power level of 1~10W which is appropriate for Cubesat[4]. Additionally, the μVAT is uniquely suited for CubeSat because of their simple, scalable, and robust construction[5].

Several different designs of the μVAT have been developed, and two basic types of them are the ring-electrodes μVAT and the co-axial μVAT[6], as shown in Fig.1. The ring-electrodes μVAT consists of an annular cathode, a similar diameter annular anode and an annular insulator between the electrodes. The co-axial μVAT employs cylindrically shaped cathode and anode instead of the ring electrodes. In this paper we consider both the ring-electrodes μVAT and the co-axial μVAT.

The μVAT operates in pulsed mode. In one discharge process, an electric arc between the cathode and the anode is formed and erodes the electrode material, mainly the cathode, producing highly-ionized plasma, and then the plasma is accelerated and expands through the channel, with the generation of thrust. The localized spots formed on the cathode surface from which the arc originates are known as cathode spots. A simple model of the vacuum-arc cathode-spot and plasma region was developed to predict the performance of the thruster, but influences of the thruster geometry and magnetic field were not considered[7].

A widely-known fact is that the thruster performance can be improved with an applied axial magnetic field. It has been found that the magnetic field can increase the specific impulse, and improve the uniform erosion of the cathode, which is critical for ensuring a long lifetime[8]. A hydrodynamic model was applied to calculate the plasma jet profile, and the results showed that with the magnetic field increase, the ion current fraction increases and the plume expansion decreases[9]. These are also in good agreement with the experimental data. The ion velocity in the μVAT was studied by Taisen Zhuang et al. using Langmuir probes[10], and the results showed that the magnetic field can lead to significant ion acceleration in the vacuum arc plasma jet, and the acceleration occurs in the divergent part of the magnetic field. The μVAT plasma plume was also studied, and it is found that the strong magnetic field can lead to hollow plume formation[11]. However, the acceleration mechanism with the magnetic field was still unclear. A numerical analysis performed by Lubos Brieda et al. with PIC method has got some preliminary results[12], indicating that the electric field due to the magnetized electrons is responsible for turning and ejecting ions from the device, and the device thrust is governed by diffusion in the absence of a magnetic field.

From the researches above, it is indicated that the simulation of the μVAT plume structure is not enough. And it is worth to discuss other factors which will affect the plume structure. In this paper, more simulations based on PIC

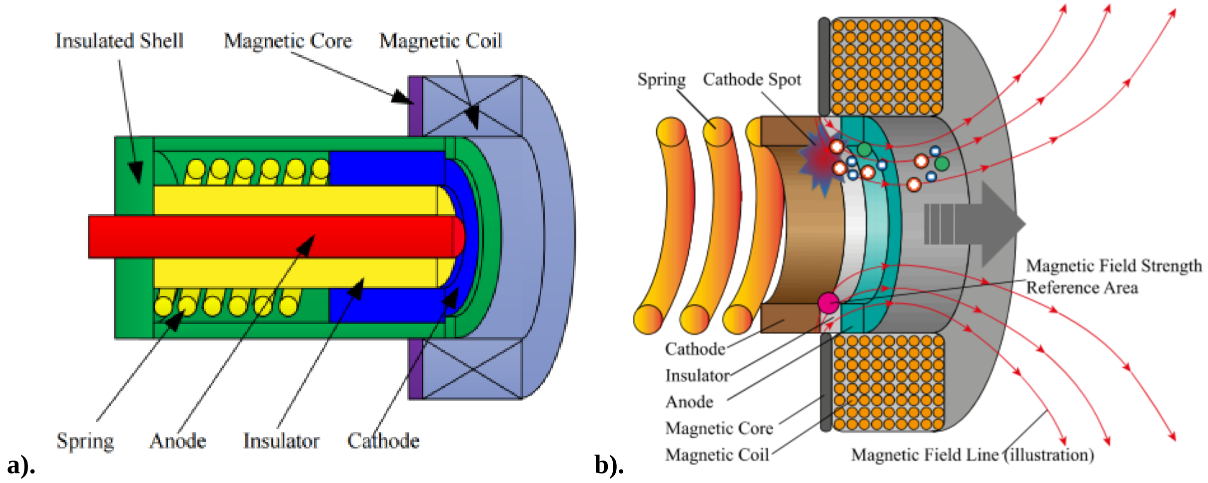

Figure 1. Schematic of the μVAT: a). the ring-electrodes μVAT; b). the co-axial μVAT.

method will be performed to study the μVAT plume. A 2D axisymmetric thruster model will be built, and then the influences of the magnetic field intensity on the plasma plume will be discussed. Both the ring-electrodes μVAT and the co-axial μVAT will be studied.

II.Method

A. PIC Method

The Particle-In-Cell (PIC) method is an efficient numerical method for plasma simulation. In this method, the charged particles are moving in the self-consistent electric field calculated on a spatial grid from the Poisson equation, while one particle may represents many real particles. The PIC method typically includes the following procedures:

Solving the equations of motion; Interpolating the charge and current source terms to the field mesh; Computing the fields on mesh points; Interpolating the fields from the mesh to the particle locations; Dealing with other problems such as ionization, collision and so on.

In this work, only ions and electrons are considered for the vacuum arc plasma is highly ionized[7]. Meanwhile, the collisions (ion-ion, electron-electron and ion-electron) in the plasma are all ignored. The applied magnetic field intensity in the thruster is much greater than the self-induced one so that the magnetic field is set to be constant. The movement of the particles is described by Newton-Lorentz equation [Eqs. (1)-(2)], and the potential is calculated by solving Poisson equation [Eq. (3)].

$$\frac{\mathrm{d}}{\mathrm{d}t} m\boldsymbol{v} = q\left(\boldsymbol{E} + \boldsymbol{v} \times \boldsymbol{B}\right) \tag{1}$$

$$\frac{\mathrm{d}}{\mathrm{d}t} \boldsymbol{x} = \boldsymbol{v} \tag{2}$$

$$\nabla^2 \phi = -\frac{\rho}{\varepsilon} \tag{3}$$

Additionally, the plasma is supposed to be isothermal, so the temperature of particles remains constant.

B. Scaling Scheme

The time step of the simulation is limited by the cyclotron frequency of electrons, while the latter is in the order of 10^{11}Hz in the magnetic field of 0.4T. However, if the time step is set to 10^{-12}s, the computing workload would be excessive and make the simulation unrealistic. Although the method of reduced ion mass and larger vacuum permittivity has been used to reduce the computations, the results were not accurate for the material properties have been changed. In this work, a scaling method put forward by Prof. Taccogna is performed to scale down the model size and speed up the convergence[13]. The correlations between the parameters must remain the same when the scaling method is applied, as shown in Table.1.

Table 1. Summary of the scaling laws (unscaled quantities are designated with asterisk)

Quantities	Scaling scheme
length	$L=\xi L^*$
velocity	$V=V^*$
mass flow rate	$\dot{m}=\xi^2 \dot{m}^*$
density	$n=n^*$
current	$I=\xi^2 I^*$
magnetic field intensity	$B=\xi^{-1} B^*$

C. Simulation Initialization

The simulation domains are 2-D axisymmetric and consist of the cathode, insulator, anode and the shell, as shown in Fig. 2, for the ring-electrodes μVAT and the co-axial μVAT respectively. The particle's position is 2-D, while the velocity is still 3-D because of the existence of the magnetic field. The magnetic field was calculated by FEMM software and then imported into the PIC program. Simulations of the two types of μVAT used the same magnetic field profile, which is shown in Fig.3. The magnetic field $\boldsymbol{B}$ could be simply changed by multiplying a factor of 0-1 at every grid when needing to discuss its influences on the plasma. Here, we set the values of the factor to 0, 0.03, 0.1, 0.3, 0.5 and 1 respectively.

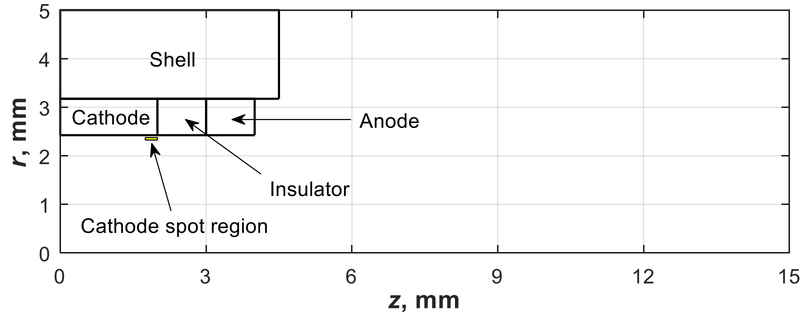

a).

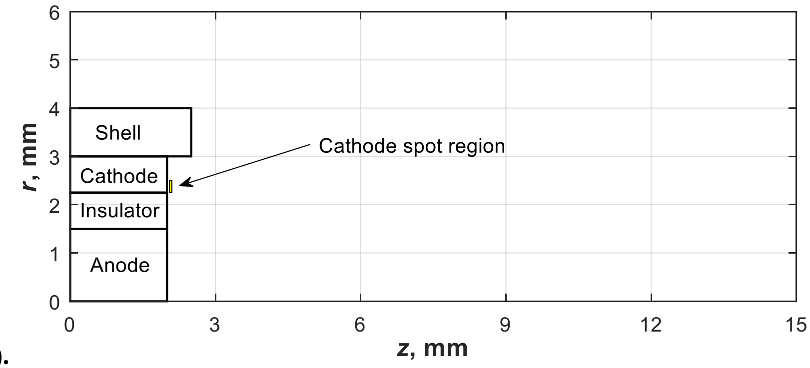

b).

Figure 2. The simulation domains: a). the ring-electrodes μVAT; b). the co-axial μVAT.

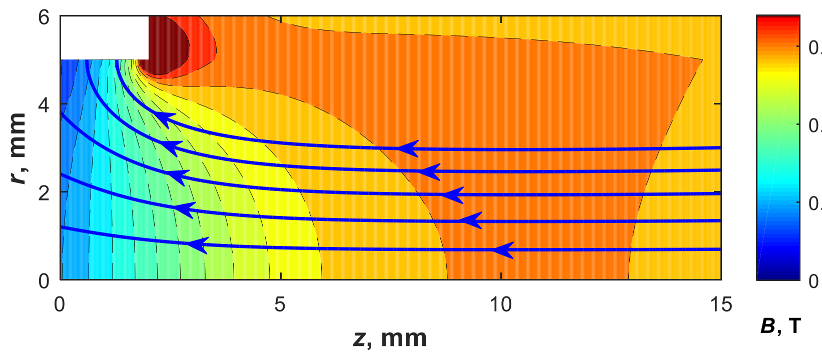

Figure 3. The magnetic field configuration. The blue lines represent the magnetic field lines.

The sizes of cathode spots in arc discharges are expected to be in sub-millimeter rage that typical spot radius is 50 μm. And the density of the plasma just produced in the cathode spot will be on the order of 10^{26}m^{-3}, which is beyond the scope of PIC method. In the simulation, the plasma was supposed to have been expanding when entering the simulation domain, and thus the inlet zone width was set as 250μm. The mass flow rate was determined using the same way as in Ref.12, based on the steady state approximation. The simulation includes electrons, Ti^{2+} ions. The velocity distribution of electrons is assumed to be Maxwell, when the velocity of ions has a constant value but random directions. The velocity distribution of ions is showed in the following.

$$\begin{aligned} V_{iz} &= V_{i0}\cos(\theta_1)\sin(\theta_2) \\ V_{ir} &= V_{i0}\cos(\theta_1)\cos(\theta_2) \\ V_{i\theta} &= V_{i0}\sin(\theta_2) \end{aligned} \tag{4}$$

Where θ_1 and θ_2 are random numbers, and $-\pi<\theta_1<0$ for the ring-electrodes μVAT, $-\pi/2<\theta_1<\pi/2$ for the ring-electrodes μVAT, and $-\pi/2<\theta_2<\pi/2$ for both.

Table.2 gives the basic simulation parameters, where the value of ions velocity referring to Ref.7. From these it can be estimated that about 15,000 steps are needed for the ions flow to be fully developed.

In the field solver, the cathode, insulator and anode were all set to be the Dirichlet boundaries, with other boundaries in the domain set to be Neumann ones. The influence of the shell was ignored. As for the kinetic treatment, all the particles will be reflected by the axis and absorbed by the others.

Table 2. Basic parameters of the simulation

Parameters	Actual value
scale factor	ξ =0.04
inlet zone width	d=250μm
Ti^{2+} mass flow rate	$\dot{m}$=1.13x10^{-7}kg/s
cathode potential	$V_{cathode}$=0V
insulator potential	$V_{insulator}$=25V
anode potential	V_{anode}=50V
electron temperature	T_e=2eV
Ti^{2+} initial velocity	V_{i0}=16285m/s
maximum magnetic field intensity	B_{max}=0.34T
time step	$\Delta t=1\times10^{-12}$s
grid size	Δx=25um

III.Results

A. Near Plume of The Ring-electrodes μVAT

Figure.4 shows the near plume simulation results of the ring-electrodes μVAT with the basic simulation parameters, including the potential, the ions number density and the electrons number density. The magnetic field is strong enough to bind the electrons. The electrons produced in the cathode spot appear to form a thin belt, gyrating around the magnetic field line, and leading to an obvious electron region where electron density is much higher than ion density, so that a low potential channel is created in the plume. Outside the channel, the potential is much higher than that in the channel. There are two high potential areas in the plume. One is related to the anode and the other one locates in the central axis which is caused by the ion movement. Due to these two high potential areas, most ions moves into the low potential channel when leave the cathode spot region. From the distribution of ions, it is indicated that the low potential region has a significant role in guiding ions to the far-field of the thruster and thus, generating thrust. However, the fraction of ions loss in the insulator, anode and left boundary is great and can't be neglected. So a more rigorous model with detailed surface processes will be required for accurately estimating the thrust.

B. Influences of Magnetic Field Intensity

The simulation results of near plume with different magnetic field intensity are shown in Figs. 5-7. Six additional cases are considered including $\boldsymbol{B}_1=\boldsymbol{0}$, $\boldsymbol{B}_2=0.03\boldsymbol{B}$, $\boldsymbol{B}_3=0.1\boldsymbol{B}$, $\boldsymbol{B}_4=0.3\boldsymbol{B}$and $\boldsymbol{B}_5=0.5\boldsymbol{B}$, where $\boldsymbol{B}$ is the original magnetic field as mentioned above. As the magnetic field intensity reduces, the width of the electron region gets larger until it disappears. The region would disappear from the cathode spot first, for the magnetic field intensity near the cathode spot is smaller than other region. When the magnetic field intensity is lower than a certain value, it can no longer limit the movement of the electrons. At this point, the electron trajectory is mainly determined by the anode and the local plasma potential. It can be seen from Fig. 6 that many electrons begin to move around the anode.

The change of the electron region leads to the electron density reduction. The high potential region around anode the gradually connects to that of the virtual anode on the center axis, cutting off the low potential channel. At last, the low potential channel disappears, as shown in Fig. 5.

Besides, when the magnetic field intensity is lower, the electron region becomes unstable, which appears as fluctuation of the narrow region. But it was inferred that the instability has little direct effects on the motion of ions, for the latter is much too slow.

The change of the low potential channel can also be inferred from the ion density distribution, as shown in Fig. 7. The region of the high ion density narrows to the cathode spot as the magnetic field intensity decreases. When the value drops lower than 0.0375T, the ions no longer exhibit obvious directional motion. The ions will be mainly blocked by the anode and move to the center axis, resulting in a clear divergence angle of the plume. The divergence varies with the magnetic field intensity, and is minimal in the original magnetic field.

C. Results of The Co-axial μVAT

The simulation results of the co-axial μVAT, as shown in Figs. 8-11, are similar to those of the ring-electrodes μVAT. Under a strong magnetic field, the electrons are confined within a narrow channel along the field line, resulting in a region of large negative charge. And most of the ions are accelerated through the electron region, and expelled. The width of the electron region widens as the magnetic field weakens. However, it can be seen that many ions move oppositely after crossing the shell, which would cause loss of thrust and more importantly, plume contaminant to the satellite. This back flow appears on most cases, and seems hard to be prevented. It's also related to the set of initial velocity of ions and could be further studied.

IV.Conclusion

In this paper, 2-D axisymmetric PIC simulations were used to determine the influence of the applied magnetic field on the plasma plume of the μVAT. Both the ring-electrodes μVAT and the co-axial μVAT were considered. In agreement with previous results[12], a low potential channel caused by magnetized electrons was observed, and ions were guided through the channel and expelled out. It was found that the width of the electron region increases as the magnetic field weakens. For the ring-electrodes μVAT, a minimum divergence of ions flow was obtained when the magnetic field reached the maximum. However, there exists a reverse flow region in the co-axial μVAT for almost all cases, which would affect the amount of thrust and cause contamination. The instability of the electron region under a weak magnetic field was also observed.

A more detailed model with the surface process, an external circuit and a larger simulation domain is expected for the deeper investigation of the plasma structure and performance of the thruster.

Acknowledgments

This work was funded by The Foundation of China Academy of Space Technology under Grant YJJ0701 and YSC0716.

References

[1]Piattoni, J., Candini, G. P., Pezzi, G., Santoni, F., and Piergentili, F., "Plastic CubeSat: An Innovative and Low-cost Way to Perform Applied Space Research and Hands-on Education," *Acta Astronautica*, Vol. 81, No. 2, 2012, pp. 419-429.

[2]Lun, J., "Development of A Vacuum Arc Thruster for Nanosatellite Propulsion," Master Dissertation, Stellenbosch University, Stellenbosch, South Africa, 2009.

[3]Anders, A., Schein, J., and Qi, N., "Pulsed Vacuum-arc Ion Source Operated with A "Triggerless" Arc Initiation Method," *Review of Scientific Instruments*, Vol. 71, No. 2, 2000, pp. 827-829.

[4]Schein, J., Gerhan, A., Rysanek, F., and Krishnan, M., "Vacuum Arc Thruster for CubeSat Propulsion," *28th International Electric Propulsion Conference*, 2003, IEPC-2003-070.

[5]Kronhaus, I., Laterza, M., and Maor, Y., "Inline Screw Feeding Vacuum Arc Thruster," *Review of Scientific Instruments*, Vol. 88, No. 4, 2017, 043505.

[6]Kolbeck, J., Keidar, M., and Anders, A., "Micro-propulsion Based on Vacuum Arcs: A Review of Physics and Technology," *52nd AIAA/SAE/ASEE Joint Propulsion Conference*, 2016, AIAA-2016-5040.

[7]Lun, J., Dobson R. T., and Steyn, W. H., "Determining Vacuum-Arc Thruster Performance Using a Cathode-Spot Model," *Journal of Propulsion & Power*, Vol. 26, No. 4, 2010, pp. 663-672.

[8]Keidar, M., Haque, S., Zhuang, T., Shashurin, A., Chiu, D., Teel, D., Agasid, E., Tintore, O., and Uribe, E., "Micro-Cathode Arc Thruster for PhoneSat Propulsion," *27th AIAA/USU Conference on Small Satellites*, 2013, SSC-13-VII.

[9]Keidar, M., Schein, J., Wilson, K., Gerhan, A., Au, M., Tang, B., Idzkowski, L., Krishnan, M., and Beilis, I., "Magnetically Enhanced Vacuum Arc Thruster," *Plasma Sources Science and Technology*, Vol. 14, No. 4, 2005, pp. 661-669.

[10]Zhuang, T., Shashurin, A., Beilis, I., and Keidar, M., "Ion Velocities in A Micro-cathode Arc Thruster," *Physics of Plasmas*, Vol. 19, No. 6, 2012, 063501.

[11]Zhuang, T., Shashurin, A., and Keidar, M., "Micro-cathode Thruster Plume Characterization," *IEEE Transactions on Plasma Science*, Vol. 39, No. 11, 2011, pp. 2936-2937.

[12]Brieda, L., Zhuang, T., and Keidar, M., "Towards Near Plume Modeling of a Micro Cathode Arc Thruster," *49th AIAA/SAE/ASEE Joint Propulsion Conference*, 2013, AIAA-2013-4120.

[13]Taccogna, F., Longo, S., Capitelli, M., and Schneider, R., "Self-similarity in Hall plasma discharges: Applications to particle models," *Physics of Plasmas*, Vol. 12, No. 5, 2005, 053502.

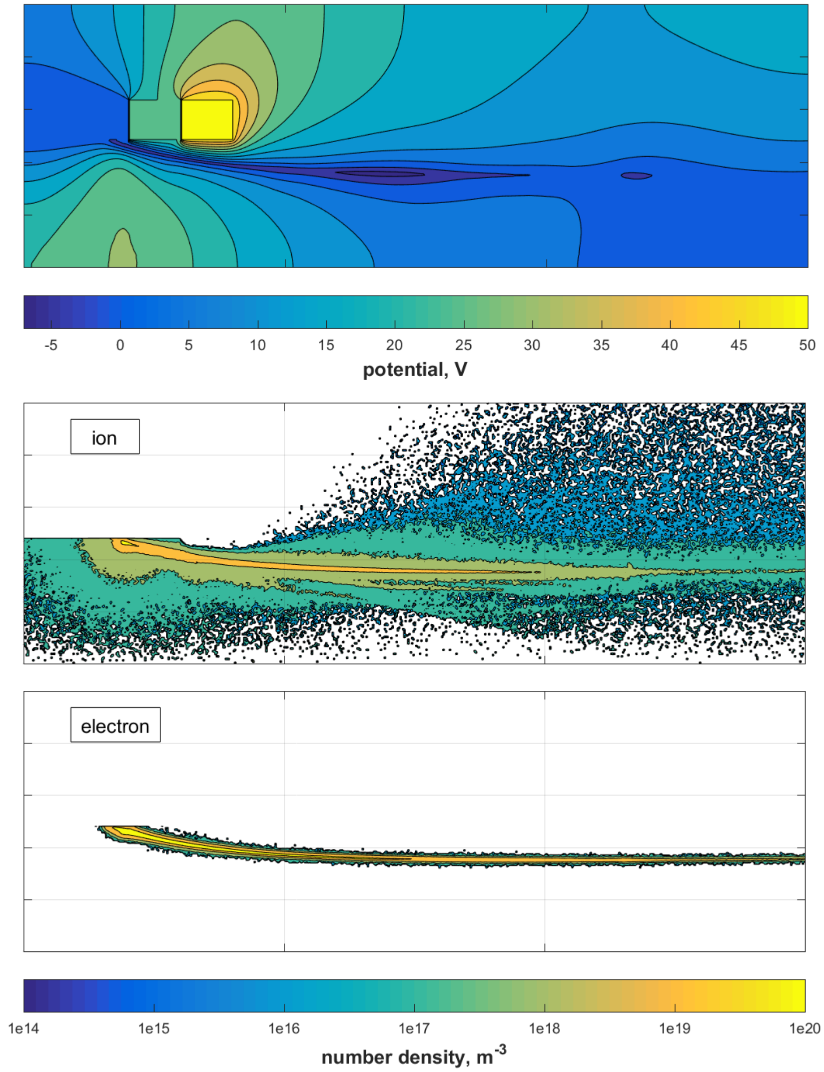

Figure 4. Simulation results of the ring-electrodes μVAT with the basic simulation parameters. B_{max}=0.34T.

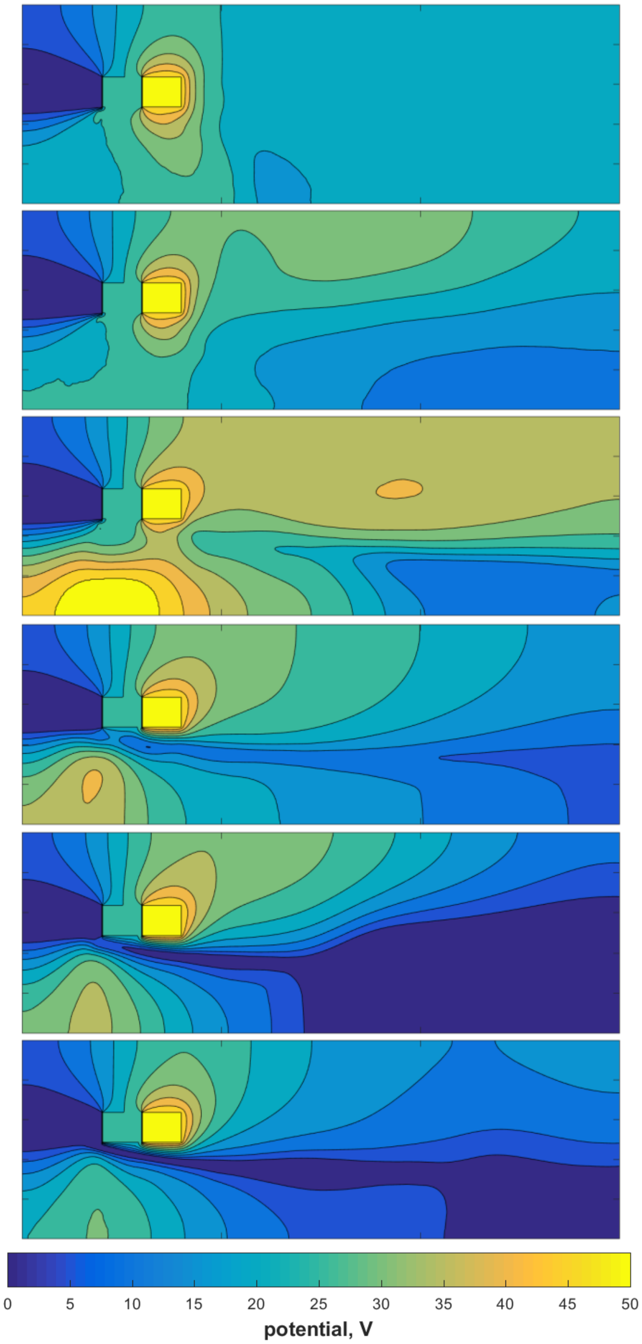

Figure 5. Potential distributions of the ring-electrodes µVAT with different magnetic fields. From top to bottom are 0, 0.003*B*, 0.1 *B*, 0.3 *B*, 0.5 *B* and *B*, where *B* is the original field.

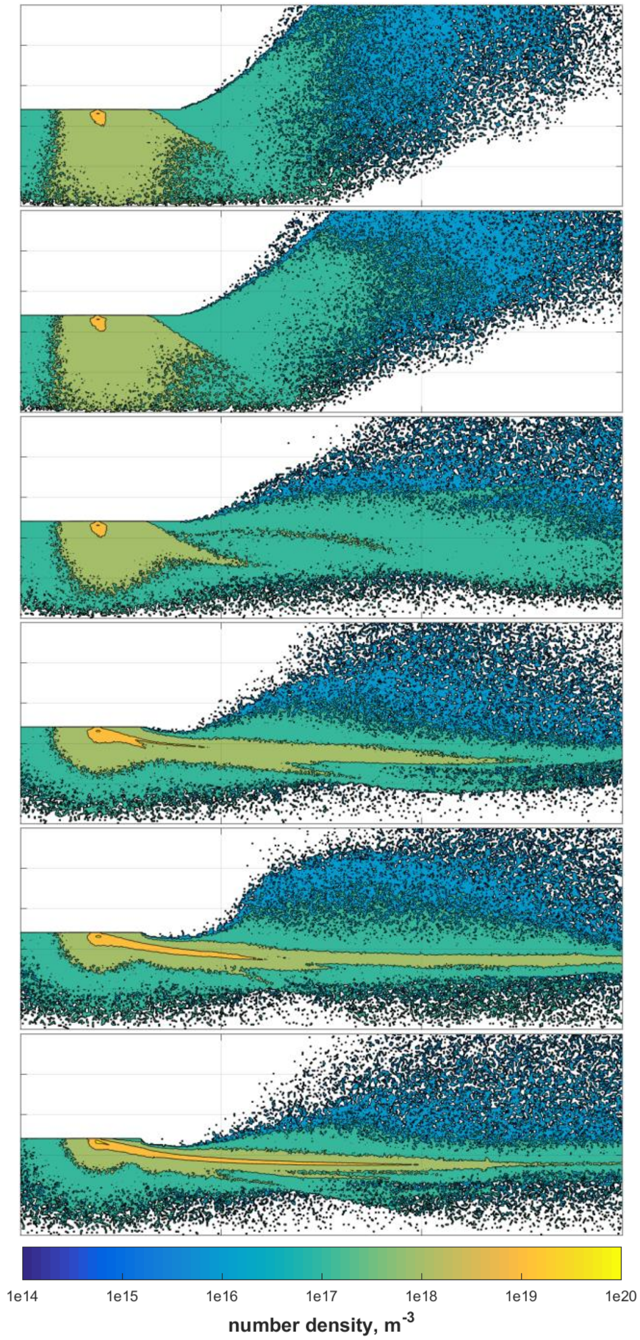

Figure 6. Ion density distributions of the ring-electrodes µVAT with different magnetic fields. From top to bottom are 0, 0.003*B*, 0.1 *B*, 0.3 *B*, 0.5 *B* and *B*, where *B* is the original field.

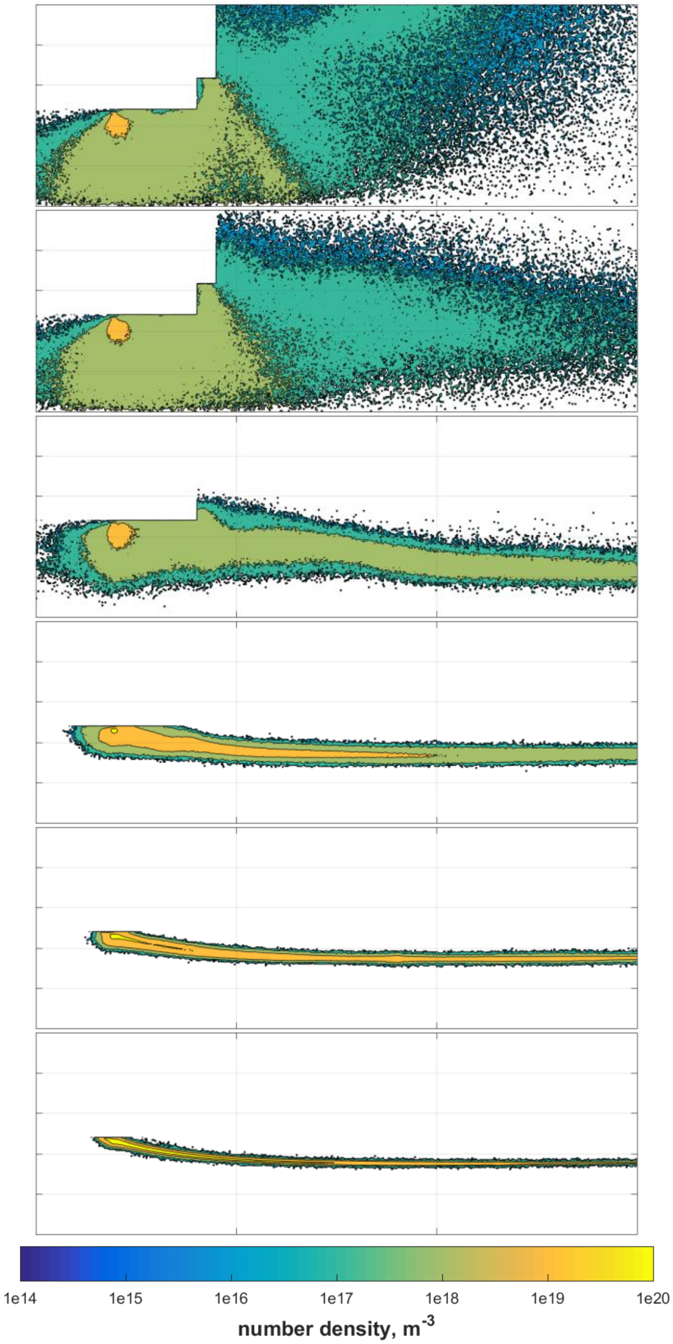

Figure 7. Electron density distributions of the ring-electrodes μVAT with different magnetic fields. From top to bottom are 0, 0.003*B*, 0.1 *B*, 0.3 *B*, 0.5 *B* and *B*, where *B* is the original field.

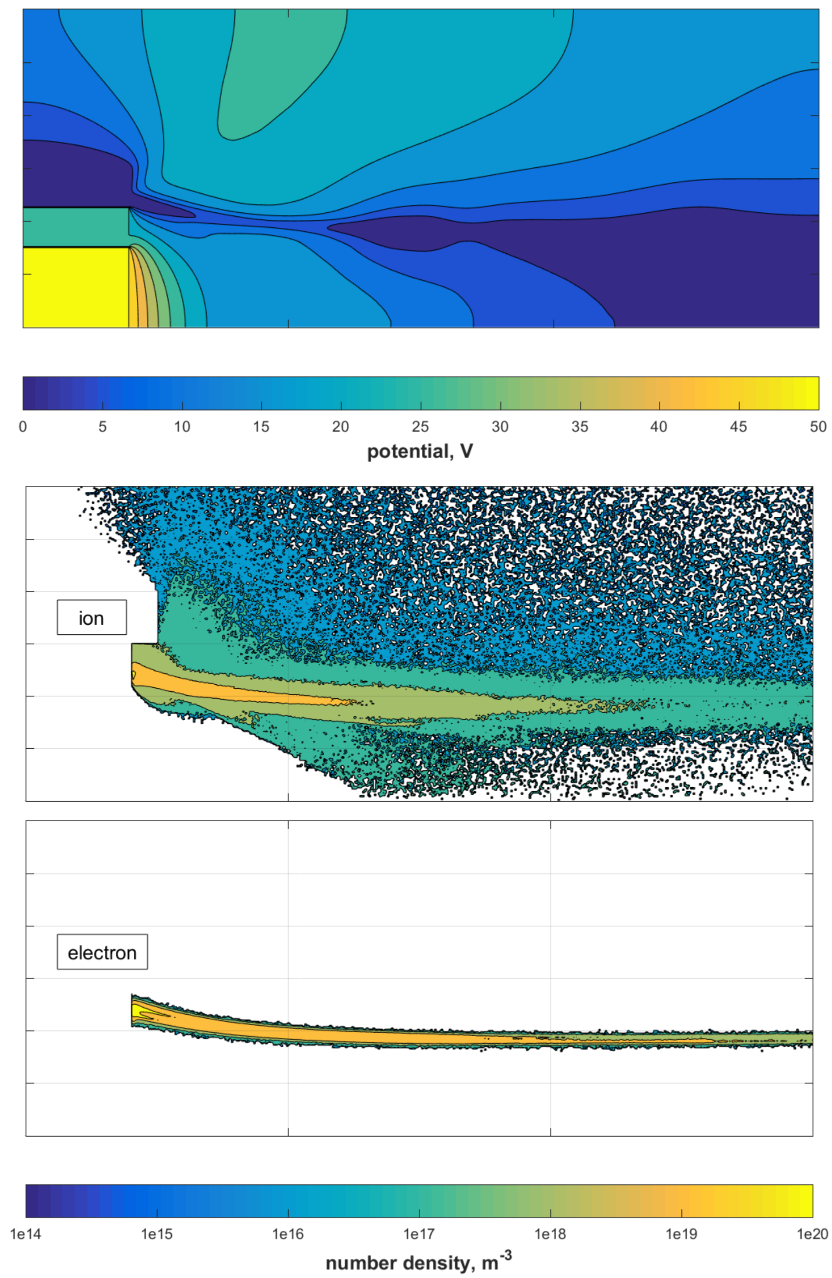

Figure 8. Simulation results of the co-axial μVAT with the basic simulation parameters. B_{max}=0.34T.

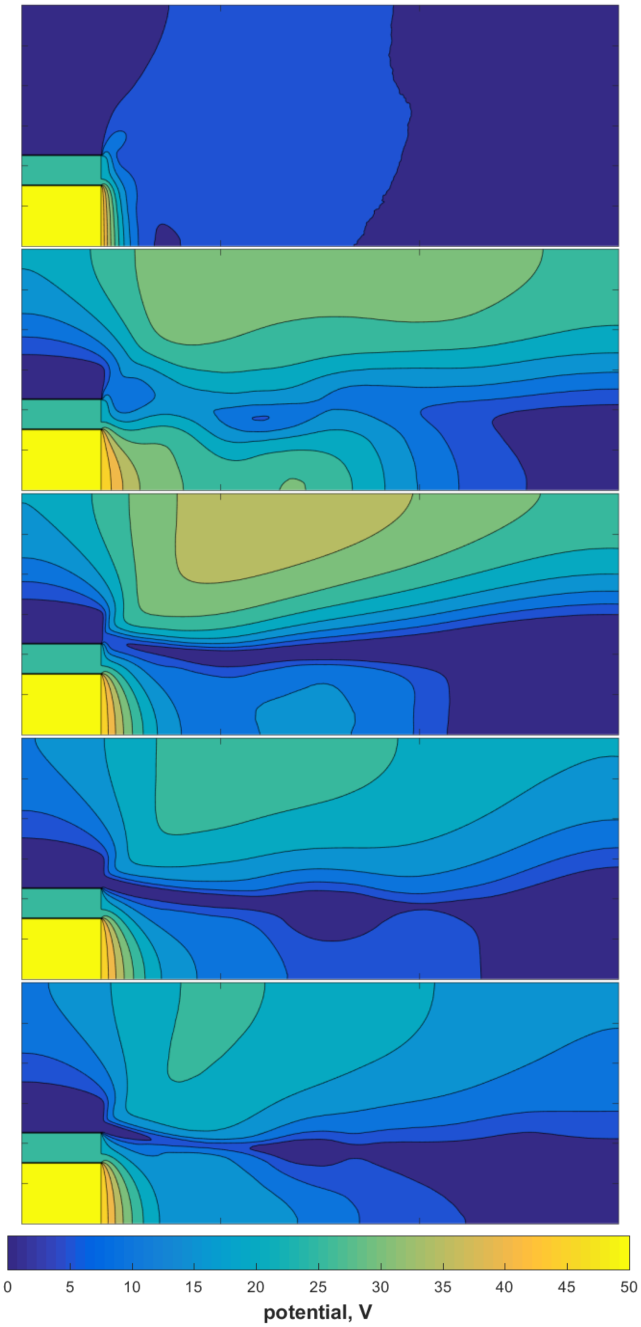

Figure 9. Potential distributions of the co-axial μVAT with different magnetic fields. From top to bottom are 0, 0.1 *B*, 0.3 *B*, 0.5 *B* and *B*, where *B* is the original field.

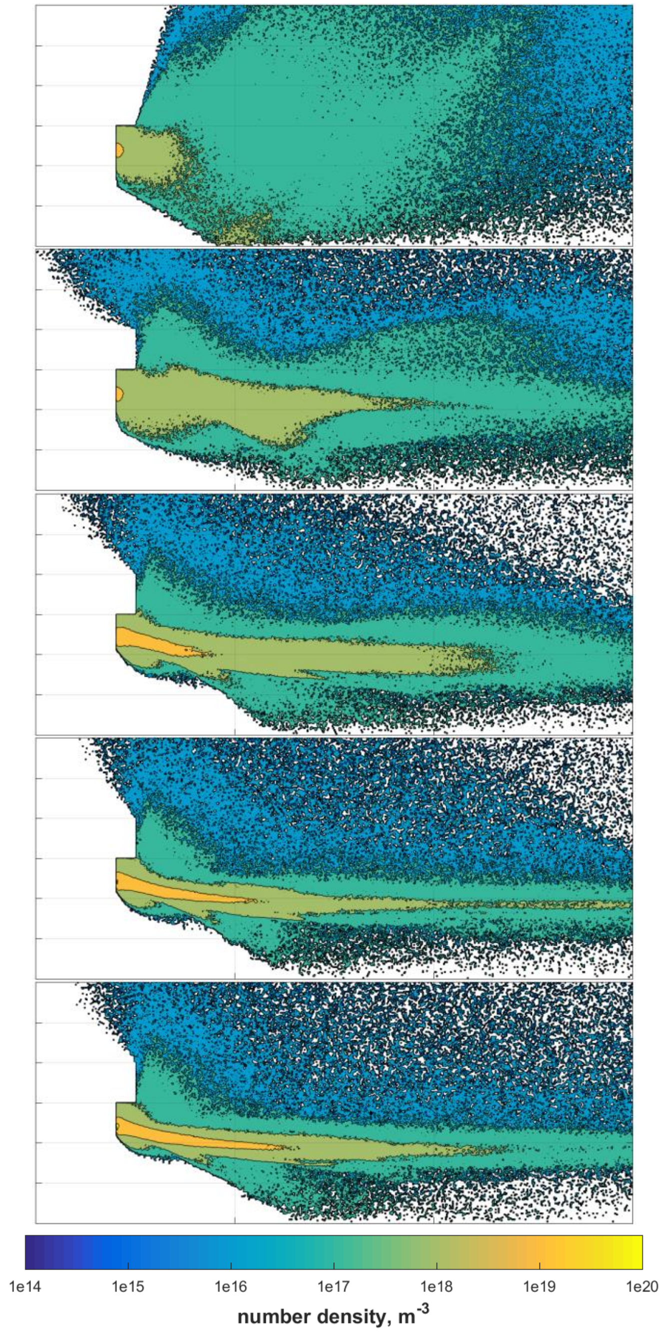

Figure 10. Ion density distributions of the co-axial μVAT with different magnetic fields. From top to bottom are 0, 0.1 *B*, 0.3 *B*, 0.5 *B* and *B*, where *B* is the original field.

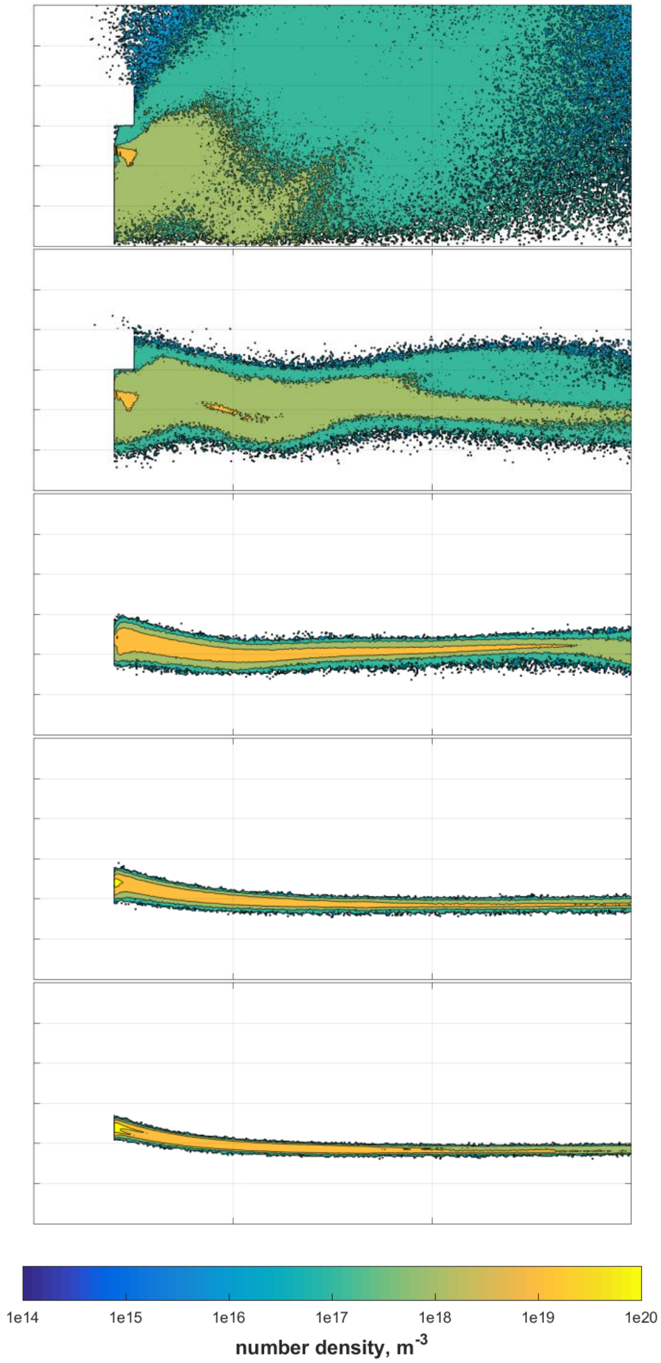

Figure 11. Electron density distributions of the co-axial μVAT with different magnetic fields. From top to bottom are 0, 0.1 *B*, 0.3 *B*, 0.5 *B* and *B*, where *B* is the original field.